IEEE Access
Multidisciplinary | Rapid Review | Open Access Journal

Received 23 August 2022, accepted 30 October 2022, date of publication 3 November 2022, date of current version 8 November 2022.

Digital Object Identifier 10.1109/ACCESS.2022.3219069

RESEARCH ARTICLE

Enhancing the Accuracy of an Explicit Solar Cell I-V Model via Low-Complexity Search-Based Parameter Extraction

HENRIQUE P. CORRÊA AND FLÁVIO H. T. VIEIRA
School of Electrical, Mechanical and Computer Engineering, Federal University of Goiás, Goiânia 74605-010, Brazil
Corresponding author: Henrique P. Corrêa (pires_correa@ufg.br)

ABSTRACT A new approach for extracting parameters of the recently introduced explicit two-piece quadratic model (ETPQM) for solar cell current-voltage (I-V) characteristics is proposed. It consists in introducing a new I-V point condition which enables expressing all ETPQM parameters as functions of an auxiliary parameter belonging to a subset of the unit interval, whose optimal value is then found by means of a low-complexity search procedure. The proposed approach is validated for different solar cells via performance (i.e., accuracy and execution time) comparisons against analytical ETPQM parameter extraction and similar low-complexity search-based methods applicable to the one-diode model (ODM). Obtained results show that the proposed method consistently outperforms the original analytical ETPQM parameter extraction in terms of accuracy. Furthermore, when compared to the low-complexity ODM-based methods, it: (i) approaches and, in some cases, surpasses their accuracies; (ii) yields much smaller execution time; and (iii) avoids the problem of wrong maximum power point fitting that may occur when using the considered low-complexity ODM-based methods.

INDEX TERMS Solar cell, modeling, parameter extraction, curve fitting.

I. INTRODUCTION

Usage of the one-diode model (ODM) for the modeling of solar cell current-voltage (I-V) characteristics has become a staple approach due to its advantages of high accuracy and physically meaningful model parameters [1], [2]. In particular, the latter feature makes it an indispensable tool for calculations during the practical design of solar cells [3].

Despite its usefulness, some criticisms to the ODM have emerged in the literature with regard to its application in higher-level (i.e., not cell design) circuit analysis. It has been argued that, in such scenarios, the modeling priority lies in obtaining explicit I-V models whose parameters can be extracted either analytically or via trivial optimization procedures, regardless of whether such parameters provide any direct physical meaning [4]. It is well-known that such requirements are not satisfied by the ODM, since it is an implicit model [i.e., $I = g(V, I)$] and the extraction of its parameters is far from straightforward. A confirmation of this latter fact is given by the sheer number of existing methods for ODM parameter extraction, each of which establishes a different compromise between accuracy of the I-V curve fitting and required computational processing [5].

To provide some brief context on existing ODM parameter extraction procedures, we draw attention to the two dominant general approaches. One of them consists in making use of simplifying approximations to compute all parameters in terms of three so-called remarkable operating points (open circuit, short circuit and maximum power); methods of this type [6], [7], [8], [9], [10] are less accurate but very fast due to being analytical. The other general approach is using multivariable optimization to compute ODM parameters via minimization of root mean square error (RMSE) of the predicted I-V curve with respect to the empirically sampled characteristic; such methods [11], [12], [13], [14], [15], [16], [17], [18], [19], [20], [21], [22], and [23] have high accuracy but require larger execution times due to the wide

The associate editor coordinating the review of this manuscript and approving it for publication was Claudia Raibulet.

five-dimensional variable domain that must be explored during optimization [24]

A third, albeit less common, type of parameter extraction approach is described as follows. First, the remarkable points are used to express some ODM parameters as functions of the remaining ones, which are treated as free parameters. Then, a low-dimensional direct search is carried out over the free parameters to minimize RMSE with respect to the empirical I-V curve. Such methods [25], [26], and [27] are more accurate than the analytical ones (due to RMSE minimization) and faster than the optimization-based ones (due to usage of low-dimensional direct search), which leads to an adequate compromise between accuracy and computational burden. At last, an added advantage is that direct search is trivial to implement. As will soon be explained, such benefits of this general approach to parameter extraction are the motivation behind the contribution proposed in this paper.

A. THE EXPLICIT TWO-PIECE QUADRATIC MODEL

Based on the aforementioned criticisms to the ODM, a number of explicit I-V models have been proposed in the literature [28], [29], [30], [31], [32], [33] to avoid its disadvantages. Such models have equations of form $I = g(V)$ whose parameters can be computed analytically from the remarkable points. In [4], a comprehensive assessment of the models from [28], [29], [30], [31], [32], and [33] was carried out. Despite concluding that the power law model [33] performs better in most cases, it was found out that all models presented significantly worsened performances for specific solar cell fill factor (FF) ranges. Taking this problem into account, we have recently proposed the explicit two-piece quadratic model (ETPQM), which was shown to always perform better or comparably to the power law model, yet with more consistency over a wide FF range [34].

For the sake of better understanding, we now recall the ETPQM formulation and the analytical parameter extraction derived for it in [34]. The I-V equation of ETPQM is:

$$I(V) = \overbrace{[aV^2 + bV + c]}^{g_I(V)} u(V - V_{mp}) + \underbrace{\left[\frac{-e - \sqrt{e^2 - 4d(f - V)}}{2d}\right]}_{h_I(V) = [g_V(I)]^{-1}} u(V_{mp} - V) \quad (1)$$

where $V \in [0, V_{oc}]$, $g_V(I) = dI^2 + eI + f$, $u(\cdot)$ is the unit step and a, b, c, d, e and f are the model parameters.

In [34], the following result was derived for computing the ETPQM parameters analytically via the remarkable points:

Proposition 1: The ETQPM parameters are given by:

$$a = \frac{I_{mp}}{(V_{oc} - V_{mp})^2} \cdot \left(\frac{V_{oc}}{V_{mp}} - 2\right) \quad (2)$$

$$b = -\frac{2V_{mp}I_{mp}}{(V_{oc} - V_{mp})^2} \cdot \left(\frac{V_{oc}}{V_{mp}} - 2\right) - \frac{I_{mp}}{V_{mp}} \quad (3)$$

$$c = \frac{I_{mp}V_{oc}}{V_{mp}} - \frac{V_{oc}I_{mp}(V_{oc} - 2V_{mp})^2}{V_{mp}(V_{oc} - V_{mp})^2} \quad (4)$$

$$d = -\frac{V_{mp}(2I_{mp} - I_{sc})}{I_{mp}(I_{mp} - I_{sc})^2} \quad (5)$$

$$e = \frac{2V_{mp}(2I_{mp} - I_{sc})}{(I_{mp} - I_{sc})^2} - \frac{V_{mp}}{I_{mp}} \quad (6)$$

$$f = \frac{V_{mp}I_{sc}(2I_{sc} - 3I_{mp})}{(I_{mp} - I_{sc})^2} \quad (7)$$

Proof: See [34]. ■

where V_{oc} is the open circuit voltage, V_{mp} is the maximum power point voltage, I_{sc} is the short circuit current and I_{mp} is the maximum power point current.

B. PROPOSED CONTRIBUTION

Recall from the previous discussion on ODM parameter extraction that the fully analytical methods are less accurate since they only consider the I-V curve remarkable points and, as a consequence, do not minimize RMSE with respect to a sampled I-V characteristic. It is clear that identical considerations apply to the ETPQM parameter extraction given by (2)-(7) and, as a consequence, we may expect that computing a, b, c, d, e and f via RMSE minimization will improve the accuracy yielded by (1).

However, note that using multivariable optimization would lead to possibly even greater execution time than in the ODM case, since we would have to deal with a six-dimensional optimization whose variables (a, b, c, d, e and f) bring the additional difficulty of not having reasonably well-known domain bounds. Hence, the remaining alternative for improving ETPQM accuracy with small execution time is to devise a low-complexity search-based parameter extraction method, similarly to those proposed in [25], [26], and [27] for the ODM.

The above discussion leads precisely to the contribution presented in this paper. A search-based method for extracting the ETPQM parameters is proposed which enhances model accuracy when compared to the original explicit equations. It consists in using a new I-V point condition that allows expressing all model parameters as functions of an auxiliary parameter which belongs to a subset of the unit interval. Hence, the ETPQM parameters are extracted via one-dimensional direct search, whose complexity is further reduced due to the narrow domain to which the auxiliary parameter belongs.

II. LOW-COMPLEXITY SEARCH-BASED PARAMETER EXTRACTION METHOD FOR THE ETPQM

The proposed parameter extraction method is derived in what follows. A scheme of (1) is given in Fig. 1, where the unused parts of curves $g_I(V)$ and $g_V(I)$ are drawn as dashed lines and the conditions pertaining to remarkable points are indicated by arrows. In the analytical method [34], we used the following conditions to compute a, b, c, d, e and f:

- $g_V(I_{sc}) = 0$ (short circuit current);
- $g_I(V_{oc}) = 0$ (open circuit voltage);

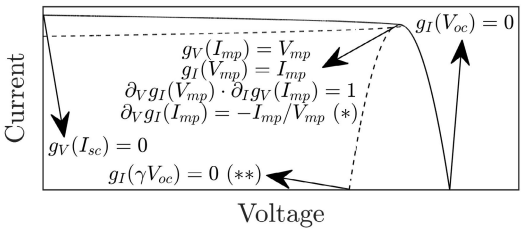

FIGURE 1. Scheme of the quadratic model. The condition marked with one asterisk is used in the original analytical method, whereas the proposed approach substitutes it by the one marked with two asterisks.

- $g_I(V_{mp}) = I_{mp}$ (maximum power current);
- $g_V(I_{mp}) = V_{mp}$ (maximum power voltage);
- $\partial_V g_I(V_{mp}) \cdot \partial_I g_V(I_{mp}) = 1$ (orthogonality);
- $\partial_V g_I(V_{mp}) = -\frac{I_{mp}}{V_{mp}}$ (maximum power derivative);

where ∂_x denotes derivative with respect to x and a total of six equations on six parameters is obtained.

In particular, the condition $\partial_V g_I(V_{mp}) = -\frac{I_{mp}}{V_{mp}}$ is less strict than the remaining ones. It only enforces a current derivate value, whereas the other conditions interpolate the remarkable points and ensure that (1) is differentiable at V_{mp}. Hence, it is proposed that this condition be substituted by $g_I(\gamma V_{oc}) = 0$, as indicated in Fig. 1, where γ is the so-called auxiliary parameter. In what follows, we show in **Lemma 1** that γ necessarily belongs to a subset of interval $[0, 1]$.

Lemma 1: $\gamma \in [0, 1]$. Moreover, if $V_{mp} \geq \frac{V_{oc}}{2}$, then we have $\gamma \in \Gamma = [0, \gamma_{\max}]$, where $\gamma_{\max} = 2V_{mp}/V_{oc} - 1$.

Proof: First, let $V_{mp} \geq \frac{V_{oc}}{2}$. From physical considerations, $\partial_V I < 0$ must be satisfied for all $V \in [0, V_{oc}]$. It is seen from Fig. 1 that this requirement is satisfied if and only if $V_{mp} - \gamma V_{oc} \geq V_{oc} - V_{mp}$, otherwise the intercept of $g_I(V)$ and $h_I(V)$ at V_{mp} would be such that $\partial_V g_I(V_{mp}) > 0$, which is not allowable. Hence, the maximum value of γ is obtained by enforcing equality, from which $\gamma_{\max} = 2V_{mp}/V_{oc} - 1$ is obtained. For $V_{mp} < \frac{V_{oc}}{2}$, it is seen from (2) that $g_I(V)$ is a convex parabola and $\partial_V g_I(V_{mp}) < 0$ is thus satisfied for any value of γ. Now, since the parabola is: (i) convex, (ii) passes through (V_{mp}, I_{mp}) and (iii) has V_{oc} as its rightmost intercept at the V-axis, it is necessary that $\gamma < 1$. ■

Since $V_{mp} > \frac{V_{oc}}{2}$ for usual cells, we see that **Lemma 1** further reduces the already narrow domain of parameter γ. We now proceed to deriving **Proposition 2**, in which the ETPQM parameters are expressed as functions of γ.

Proposition 2: Assuming the I-V quadratic model in (1), its associated parameters can be computed as:

$$a = K \cdot (I_{mp} - I_{sc}) \tag{8}$$
$$b = -K \cdot (1 + \gamma)(I_{mp} - I_{sc})V_{oc} \tag{9}$$
$$c = K \cdot \gamma (I_{mp} - I_{sc})V_{oc}^2 \tag{10}$$
$$d = K - V_{mp}(I_{mp} - I_{sc})^{-2} \tag{11}$$
$$e = 2V_{mp}I_{mp}(I_{mp} - I_{sc})^{-2} - K \cdot (I_{mp} + I_{sc}) \tag{12}$$
$$f = K \cdot I_{mp}I_{sc} + V_{mp}I_{sc}(I_{sc} - 2I_{mp})(I_{mp} - I_{sc})^{-2} \tag{13}$$

where $K = -\frac{I_{mp}}{(I_{mp}-I_{sc})(V_{mp}^2-(1+\gamma)V_{oc}V_{mp}+\gamma V_{oc}^2)}$.

Proof: By enforcing the remarkable point conditions to (1) with the derivative condition substituted by $g_I(\gamma V_{oc}) = 0$, a nonlinear system on a, b, c, d, e and f is obtained:

$$aV_{oc}^2 + bV_{oc} + c = 0 \tag{14}$$
$$a\gamma^2 V_{oc}^2 + b\gamma V_{oc} + c = 0 \tag{15}$$
$$aV_{mp}^2 + bV_{mp} + c = I_{mp} \tag{16}$$
$$dI_{sc}^2 + eI_{sc} + f = 0 \tag{17}$$
$$dI_{mp}^2 + eI_{mp} + f = V_{mp} \tag{18}$$
$$2dI_{mp} + e = 1/(2aV_{mp} + b) \tag{19}$$

The nonlinearity of (19) does not prevent the computation of a solution. To achieve this, first solve (14)-(16), which constitute a linear system on a, b and c. Then, manipulate the obtained expressions algebrically to arrive at (8)-(10). Substituting a and b into (19), it is seen that (17)-(19) become a linear system on d, e, f, which is then solved for obtaining (11)-(13) and thus completes the proof. ■

In this sense, all parameters in (1) have been expressed as functions of γ via (8)-(13). It remains to determine the optimal γ^* value, which we define as the one that minimizes normalized root mean square error (NMRSE) with respect to an empirically sampled I-V characteristic $I_{\text{ref}}(V)$. The current normalized absolute error (NAE) and NMRSE, which are henceforth denoted by ξ and Ξ, are defined as:

$$\xi(V) = \frac{1}{I_{sc}} \cdot |I(V) - I_{\text{ref}}(V)| \tag{20}$$
$$\Xi = \left[\frac{1}{N_v}\sum_{i=1}^{N_v} \xi^2(V_i)\right]^{1/2} \tag{21}$$

where V_i, $i = 1, 2, \ldots, N_v$, is the i-th sample of the empirical I-V curve. Note that, since I_{sc} is a constant, minimization of NRMSE is equivalent to that of RMSE.

Hence, we have reduced ETPQM parameter extraction to solving the single-variable optimization $\gamma^* = \text{argmin}_{\gamma\in\Gamma}\ \Xi$. Since Γ is a narrow interval (as established by **Lemma 1**), we simply propose that it be discretized according to an increment $\Delta\gamma$ and optimization be carried out via direct search over $\mathcal{G} = \{i \cdot \Delta\gamma \mid i = 0, 1, \ldots, N_\gamma\}$, where $N_\gamma = \gamma_{\max}/\Delta\gamma$. In other words, we evaluate Ξ for every $\gamma \in \mathcal{G}$ and select γ^* as the value which yields the smallest Ξ.

Remark 1: The proposed optimization uses the simplest possible implementation of direct search, which consists in searching Γ by means of fixed steps $\Delta\gamma$. This implementation is named *compass search* by some authors [35].

III. REQUIRED NUMBER OF OPERATIONS AND COMPARISON TO ODM-BASED SEARCH METHODS

We now comment on the number of operations required by the proposed method, where we count evaluation of NRMSE via (20) and (21) as the basic elementary operation. Since the method evaluates Ξ for all $\gamma \in \mathcal{G}$ and $\gamma_{\max} = \sup \mathcal{G}$, it is clear that the total number of operations is $1 + \frac{\gamma_{\max}}{\Delta\gamma}$, which has the favorable property of being linear in $\frac{1}{\Delta\gamma}$. Since $\gamma_{\max} \leq 1$, the number of operations is clearly bounded.

Furthermore, we see that the proposed method has an easily tunable trade-off between accuracy and processing time. For instance, if a premium is put on fast execution time, this can be obtained by increasing $\Delta\gamma$, which reduces the number of computations linearly at the expense of model accuracy due to a coarser search of Γ being carried out.

For the sake of comparison, consider the required number of operations in the similar low-complexity search-based ODM parameter extraction methods from [25], [26], and [27]. In [25], a single-variable search is carried out over the ODM series resistance R_s according to an increment ΔR_s; this implies linearity with respect to $\frac{1}{\Delta R_s}$, but bounds on R_s are cell-dependent and cannot be defined in a general manner.

In [26], a search over the ODM ideality factor m is carried out with increment Δm and is followed by a search over R_s. Hence, the number of operations is linear with respect to $\frac{1}{\Delta R_s}$ and $\frac{1}{\Delta m}$. Since it is known that $m \in [1, 2]$, this amounts to an expected $1 + \frac{1}{\Delta m}$ additional operations compared to [25].

On the other hand, a two-dimensional search over R_s and m is carried out in [27]. As a consequence, the number of operations is no longer linear on the increment reciprocals. Instead, it is proportional to $\frac{1}{\Delta R_s \Delta m}$, which may lead to much larger execution times for small ΔR_s or Δm.

It is thus seen that the method proposed in this work compares favorably to [25], [26], and [27] with regard to the number of required operations, since it not only is linear with respect to a single variable but, even more importantly, has general, tight and well-defined bounds on its variable γ.

IV. VALIDATION OF THE PROPOSED METHOD

The ETPQM itself has already been validated in [34] against other explicit I-V models from the literature. Hence, we focus on comparing the proposed ETPQM parameter extraction method with the analytical procedure given by (2)-(7) and with the similar ODM-based search methods from [25], [26], and [27].

A. METHODOLOGY

Validation is carried out by applying each method to five solar cells. The selected cells have distinct manufacturing technologies and very different FF values to provide a more robust assessment. The considered solar cells are as follows:

- Monocrystalline silicon, $FF = 0.773$ [36];
- Polycrystalline silicon, $FF = 0.709$ [37];
- Thin-film with germanium substrate, $FF = 0.833$ [38];
- Organic (composite polymer), $FF = 0.442$ [39];
- Organic with titanium oxide layer, $FF = 0.147$ [40].

For the computation of NRMSE, $N_v = 50$ points with approximately equal spacing were sampled graphically from the empirical I-V characteristics reported in [36], [37], [38], and [39], [40]. As additional metrics for evaluating model accuracy, we also consider the NAEs and NRMSEs of output power $P = VI$ and current derivative $\partial_V I$. Such metrics are defined as:

$$\psi(V) = \frac{1}{P_{mp}} \cdot |P(V) - P_{\text{ref}}(V)| \tag{22}$$

$$\Psi = \left[\frac{1}{N_v}\sum_{i=1}^{N_v} \psi^2(V_i)\right]^{1/2} \tag{23}$$

$$\zeta(V) = \frac{1}{|\partial_V I_{\text{ref,m}}|} \cdot |\partial_V I(V) - \partial_V I_{\text{ref}}(V)| \tag{24}$$

$$Z = \left[\frac{1}{N_v}\sum_{i=1}^{N_v} \zeta^2(V_i)\right]^{1/2} \tag{25}$$

where ψ and Ψ are power NAE and NRMSE, ζ and Z are current derivative NAE and NRMSE, $P_{mp} = V_{mp}I_{mp}$ is the cell nominal maximum power and $\partial_V I_{\text{ref,m}}$ is the maximum current derivative (in absolute value) computed for the empirical curve via backwards difference.

We consider an increment $\Delta\gamma = 0.1\%$ for carrying out direct search with the proposed method. For the ODM-based methods, $\Delta m = 0.001$ is used for the ideality factor with search bounds $m \in [1, 2]$. On the other hand, recalling that R_s is strongly cell-dependent, we use the following reasonable guesses. For the solar cells with currents in the miliampere range, $\Delta R_s = 1\ \Omega$ and $R_s \in [0, 100]\ \Omega$, whereas for those whose currents are in the ampere range, $\Delta R_s = 1\ \text{m}\Omega$ and $R_s \in [0, 100]\ \text{m}\Omega$.

B. RESULTS

The obtained results are given in Figs. 2 to 6 and Tables 1 to 5. For each solar cell, the following information is presented in the figures: (i) sample points drawn from the empirical I-V characteristic; (ii) $I(V)$, $P(V)$, $\xi(V)$, $\psi(V)$ and $\zeta(V)$ plots obtained with each parameter extraction method; and (iii) the optimization trajectory $\Xi(\gamma)$ yielded by the proposed method. The following data are displayed in the tables for each solar cell: (i) values of Ξ, Ψ and Z for each method; (ii) measured execution time for each method, in miliseconds and rounded up to the nearest integer (i.e., $\lceil T \rceil$, where T is execution time); and (iii) whether each method provided an adequate fit of the maximum power point (MPP).

Remark 2: Implementation and execution of all considered methods was carried out in MATLAB R2017b on a laptop equipped with an Intel quad-core 2.7 GHz processor and 8 GB of RAM. The processing times were measured by using the *tic/toc* commands provided by MATLAB.

Remark 3: We define the MPP fit as adequate if the estimated P-V curve has its maximum at a voltage value within a $\pm 1\%$ range of the solar cell nominal V_{mp}.

In what follows, we briefly describe the results obtained for each of the considered solar cells. Then, a discussion on the most relevant aspects of such results is carried out.

1) MONOCRYSTALLINE CELL

As depicted in Fig. 2 and Table 1, all methods were able to provide high-quality fits to the empirical I-V curve.

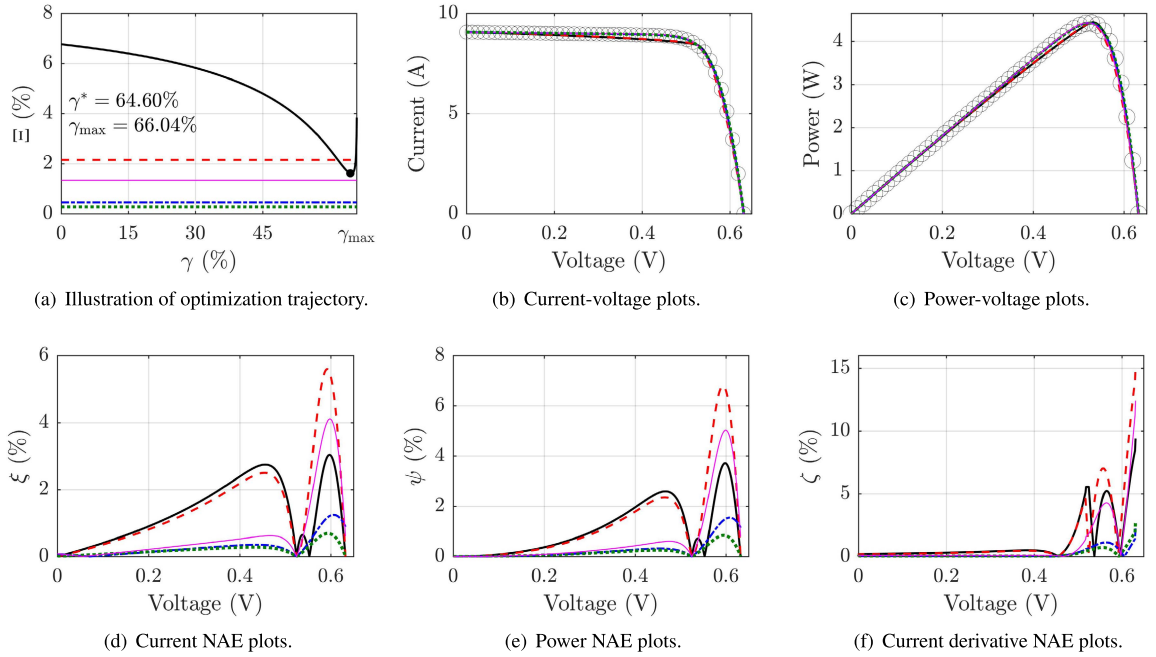

(a) Illustration of optimization trajectory. (b) Current-voltage plots. (c) Power-voltage plots.

(d) Current NAE plots. (e) Power NAE plots. (f) Current derivative NAE plots.

FIGURE 2. Obtained results for the monocrystalline solar cell, which are comprised of plots of (a) the current NRMSE optimization trajectory of the proposed method and the current NRMSE values yielded by the other considered methods, (b) I-V characteristics, (c) P-V characteristics, (d) current NAE curves, (e) power NAE curves and (f) current derivative NAE curves. The plotted curves are identified as follows: Villalva et al. [25] (thin solid line, magenta), Vieira and Corrêa [26] (alternating traced line, blue), Rhouma et al. [27], analytical method [34] (traced line, red), proposed method (solid line, black) and empirical I-V samples (gray round markers, only in I-V and P-V plots). Numerical values of current NRMSE, current derivative NRMSE, power NRMSE and execution time are given in Table 1.

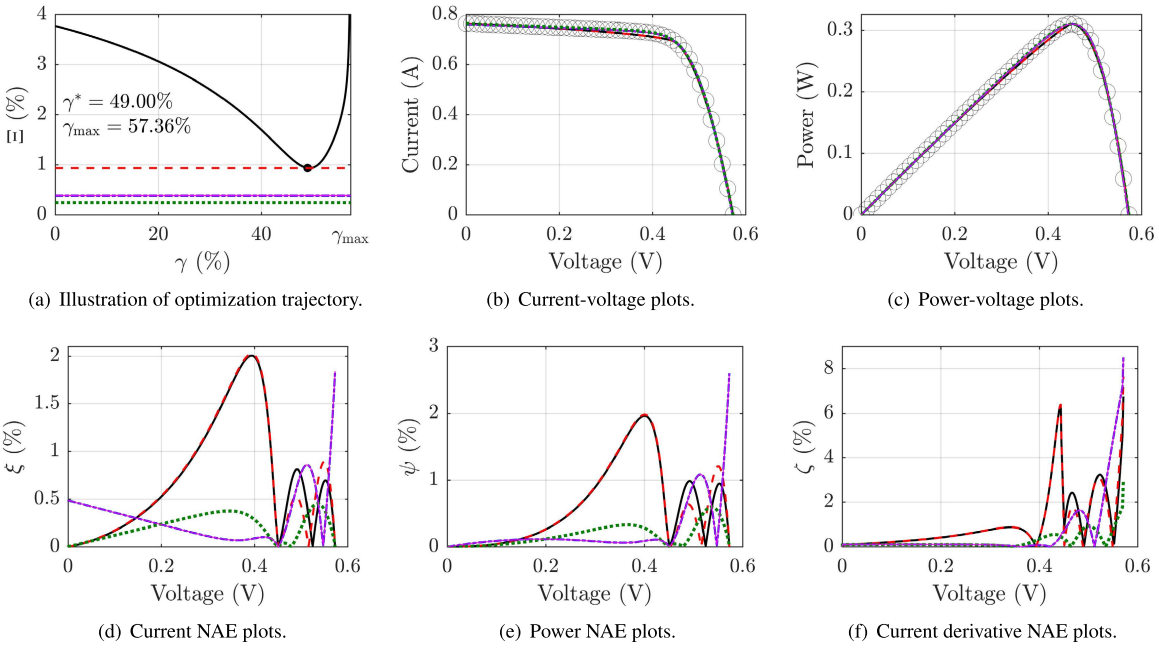

(a) Illustration of optimization trajectory. (b) Current-voltage plots. (c) Power-voltage plots.

(d) Current NAE plots. (e) Power NAE plots. (f) Current derivative NAE plots.

FIGURE 3. Obtained results for the polycrystalline solar cell, which are comprised of plots of (a) the current NRMSE optimization trajectory of the proposed method and the current NRMSE values yielded by the other considered methods, (b) I-V characteristics, (c) P-V characteristics, (d) current NAE curves, (e) power NAE curves and (f) current derivative NAE curves. The plotted curves are identified as follows: Villalva et al. [25] (thin solid line, magenta), Vieira and Corrêa [26] (alternating traced line, blue), Rhouma et al. [27], analytical method [34] (traced line, red), proposed method (solid line, black) and empirical I-V samples (gray round markers, only in I-V and P-V plots). Numerical values of current NRMSE, current derivative NRMSE, power NRMSE and execution time are given in Table 2.

The worst-performing method was the analytical ETPQM parameter extraction, which still yielded a small $\Xi \approx 2\%$. Using the proposed method, a relative NRMSE improvement of 25.08% was obtained with respect to the analytical method,

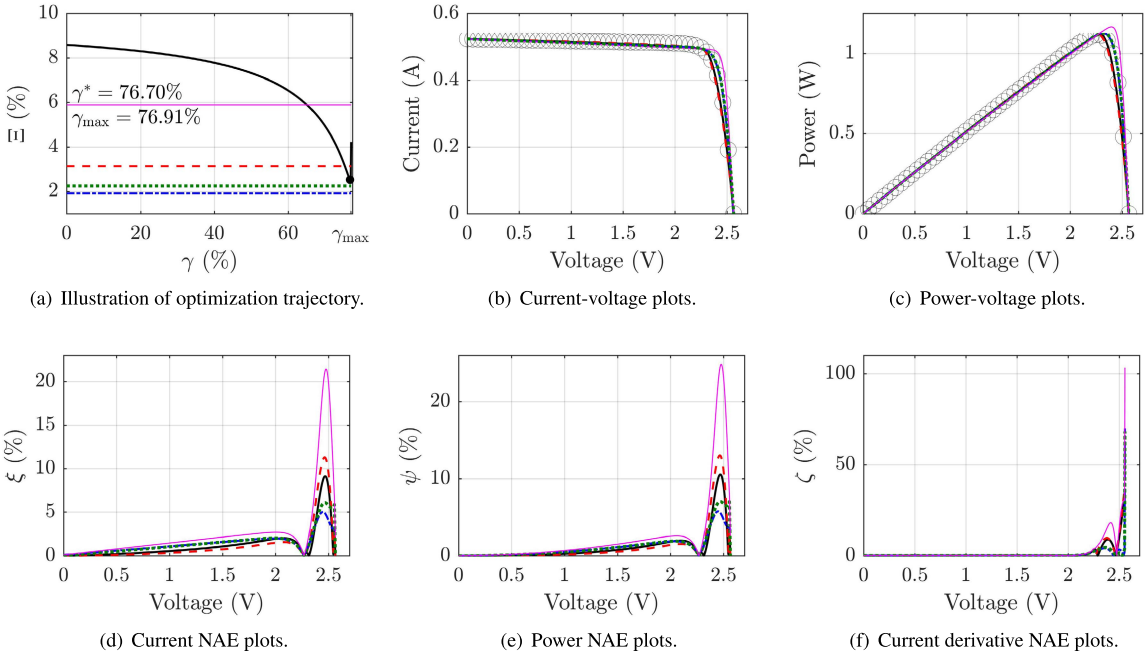

(a) Illustration of optimization trajectory. (b) Current-voltage plots. (c) Power-voltage plots.

(d) Current NAE plots. (e) Power NAE plots. (f) Current derivative NAE plots.

FIGURE 4. Obtained results for the thin-film solar cell, which are comprised of plots of (a) the current NRMSE optimization trajectory of the proposed method and the current NRMSE values yielded by the other considered methods, (b) I-V characteristics, (c) P-V characteristics, (d) current NAE curves, (e) power NAE curves and (f) current derivative NAE curves. The plotted curves are identified as follows: Villalva et al. [25] (thin solid line, magenta), Vieira and Corrêa [26] (alternating traced line, blue), Rhouma et al. [27], analytical method [34] (traced line, red), proposed method (solid line, black) and empirical I-V samples (gray round markers, only in I-V and P-V plots). Numerical values of current NRMSE, current derivative NRMSE, power NRMSE and execution time are given in Table 3.

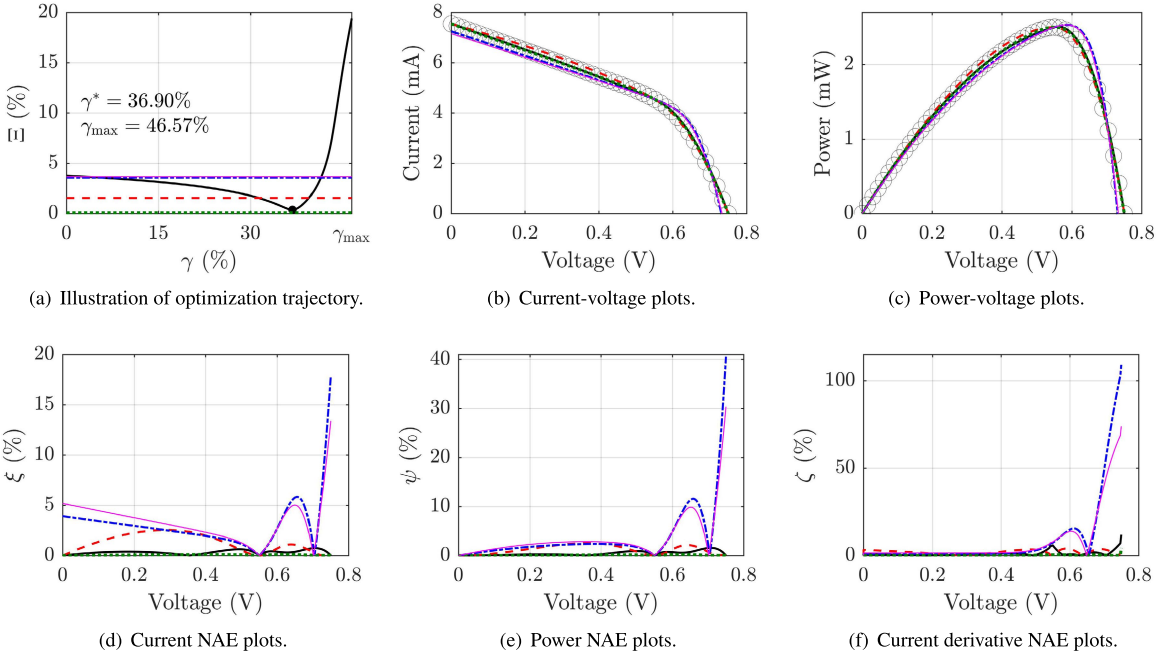

(a) Illustration of optimization trajectory. (b) Current-voltage plots. (c) Power-voltage plots.

(d) Current NAE plots. (e) Power NAE plots. (f) Current derivative NAE plots.

FIGURE 5. Obtained results for the organic solar cell, which are comprised of plots of (a) the current NRMSE optimization trajectory of the proposed method and the current NRMSE values yielded by the other considered methods, (b) I-V characteristics, (c) P-V characteristics, (d) current NAE curves, (e) power NAE curves and (f) current derivative NAE curves. The plotted curves are identified as follows: Villalva et al. [25] (thin solid line, magenta), Vieira and Corrêa [26] (alternating traced line, blue), Rhouma et al. [27], analytical method [34] (traced line, red), proposed method (solid line, black) and empirical I-V samples (gray round markers, only in I-V and P-V plots). Numerical values of current NRMSE, current derivative NRMSE, power NRMSE and execution time are given in Table 4.

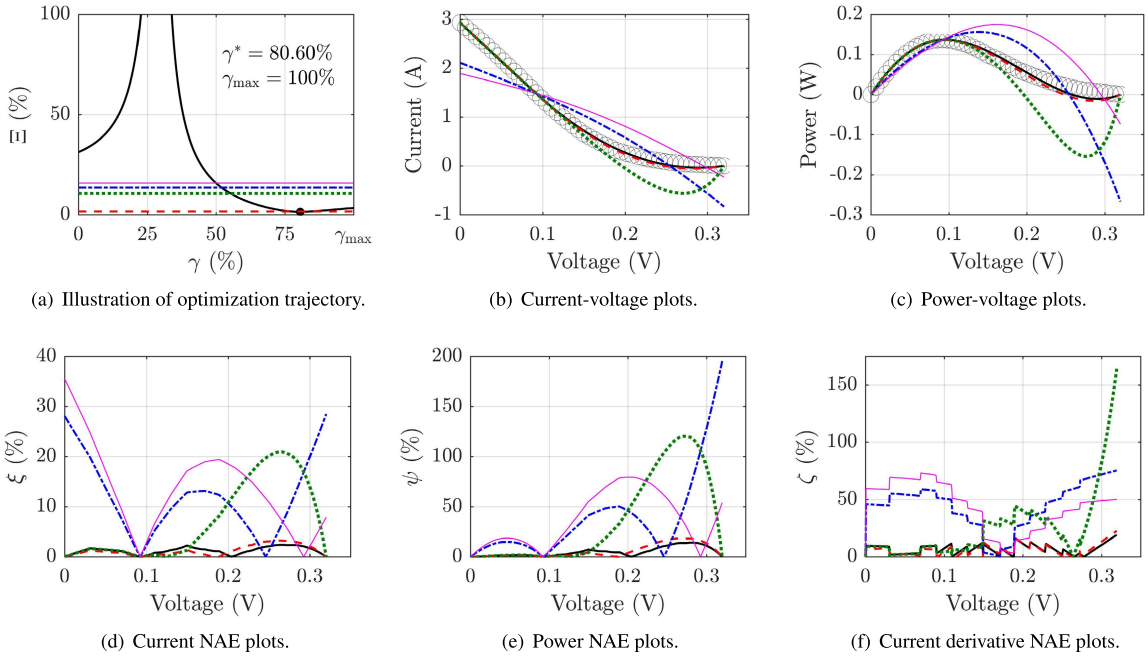

(a) Illustration of optimization trajectory. (b) Current-voltage plots. (c) Power-voltage plots.

(d) Current NAE plots. (e) Power NAE plots. (f) Current derivative NAE plots.

FIGURE 6. Obtained results for the organic solar cell with titanium oxide layer, which are comprised of plots of (a) the current NRMSE optimization trajectory of the proposed method and the current NRMSE values yielded by the other considered methods, (b) I-V characteristics, (c) P-V characteristics, (d) current NAE curves, (e) power NAE curves and (f) current derivative NAE curves. The plotted curves are identified as follows: Villalva et al. [25] (thin solid line, magenta), Vieira and Corrêa [26] (alternating traced line, blue), Rhouma et al. [27], analytical method [34] (traced line, red), proposed method (solid line, black) and empirical I-V samples (gray round markers, only in I-V and P-V plots). Numerical values of current NRMSE, current derivative NRMSE, power NRMSE and execution time are given in Table 5.

which made the proposed method very closely approach the one by Villalva et al. [25] in terms of accuracy. Together with the polycrystalline cell, this is one of the cases in which the proposed method, despite yielding low NRMSE, did not surpass the accuracy of any ODM-based method; the reason for this will be discussed in Section IV-B.6. On the other hand, it is clear that the proposed method required much smaller execution time: compared to the fastest ODM method, a 99.73% time reduction was achieved.

2) POLYCRYSTALLINE CELL

The results presented in Fig. 3 and Table 2 are similar to those for the monocrystalline cell: all methods yielded precise fits, with the worst-peforming one being, once more, the analytical method with $\Xi \approx 1\%$. The main difference in this case is that the relative NRMSE improvement by the proposed method, with respect to the analytical one, was quite modest at 0.07%. Once again, the proposed method was comparatively fast and yielded a 99.75% time reduction with respect to the ODM method with smallest execution time.

3) THIN-FILM CELL

From Fig. 4 and Table 3, it is seen that the proposed method yielded significantly superior performance to the ODM method of Villalva et al. [25] and reduced NRMSE of the analytical method by 19.62%. Furthermore, its NRMSE closely approached those of the best-performing ODM-based methods. Notably, only the proposed and analytical methods were able to adequately fit the MPP, whereas the remaining ones yielded P-V curves with large V_{mp} error. In terms of execution time, the proposed method yielded a 99.67% reduction compared to the fastest ODM-based method.

4) ORGANIC CELL

The results in Fig. 5 and Table 4 show that the proposed method attained greater accuracy than two ODM-based methods, namely those of Villalva et al. [25] and of Vieira and Corrêa [26]. It nearly equalled the performance of the ODM method of Rhouma et al. [27], yielding a very small NRMSE of $\Xi = 0.58\%$. Compared to its analytical counterpart, the proposed method yielded a large relative NRMSE improvement of 75.78%. We also note that, among the search-based methods, only the proposed method and that of Rhouma et al. [27] fitted the MPP adequately. As in previous cases, the proposed method sharply reduced execution time (by 99.84%) with respect to the fastest ODM method.

5) ORGANIC CELL WITH TITANIUM OXIDE LAYER

Some organic solar cells (such as the one with a titanium oxide layer considered here) may have severe bottlenecks in charge transport, which gives rise to physical phenomena that cause the I-V characteristic to be S-shaped and have very low *FF* [41]. This is *not* taken into account by the ODM, which may yield poor fits to experimental data [42]. Since it is not known how the ETPQM and the proposed parameter

TABLE 1. Performance metrics of each method for the monocrystalline cell.

Method	Ξ (%)	Z (%)	Ψ (%)	$\lceil T \rceil$ (ms)	MPP fit
Villalva et al. [25]	1.3282	2.1146	1.5844	2567	Adequate
Vieira and Corrêa [26]	0.4523	0.4514	0.5244	2801	Adequate
Rhouma et al. [27]	0.2757	0.3932	0.2961	24434	Adequate
Analytical method [34]	2.1539	3.1778	2.3508	1	Adequate
Proposed method	1.6136	2.1847	1.5306	7	Adequate

TABLE 2. Performance metrics of each method for the polycrystalline cell.

Method	Ξ (%)	Z (%)	Ψ (%)	$\lceil T \rceil$ (ms)	MPP fit
Villalva et al. [25]	0.3804	1.2902	0.4009	2362	Adequate
Vieira and Corrêa [26]	0.3804	1.2902	0.4009	2593	Adequate
Rhouma et al. [27]	0.2439	0.4018	0.2224	25581	Adequate
Analytical method [34]	0.9337	1.5386	0.8505	1	Adequate
Proposed method	0.9330	1.4992	0.8451	6	Adequate

extraction method would perform in this case, it must be properly assessed and compared to the ODM-based methods.

The obtained results, which are presented in Fig. 6 and Table 5, clearly show that the ETPQM is, indeed, able to fit the S-shaped characteristic much better than the ODM. In fact, the I-V curves yielded by the ODM-based methods are very innacurate, in that they have large negative-sign currents and NRMSEs above 10%. Contrastingly, the ETQPM yields $\Xi < 2\%$ both for the analytical and proposed method. As was the case for the other solar cells, the proposed method improves upon the analytical NRMSE; in this case, a relative improvement of 10.97% was obtained. At last, the proposed method has saved 99.55% execution time compared to the ODM-based method with smallest execution time.

Despite the much better performance of ETPQM and the proposed method for the S-shaped characteristic, we intend to research, in future work, further improvements specifically for S-shaped curves. In particular, the proposed method still yielded negative-sign currents (albeit in much smaller degree than the ODM-based methods) in the neighborhood of V_{oc}, which is not physically realistic. We thus conjecture that, in future work, some modification can be made to (1) so that the model itself better fits S-shaped characteristics.

6) DISCUSSION

The proposed search-based parameter extraction method consistently achieved its main objective for all solar cells, namely improving upon the NRMSE yielded by (2)-(7) with small execution time. The relative improvement with respect to analytical parameter extraction was modest in some cases but large in others, ranging from 0.07% to 75.78%.

For all non-silicon solar cells, the proposed method has surpassed at least one of the ODM-based methods and, more importantly, closely approached (and in one case surpassed) the best-performing ODM method in terms of accuracy. This confirms our initial hypothesis (see Section I-B) that, in general, the ETPQM is a high-performing explicit I-V model which could be further enhanced via optimization.

It is simple to explain why all the ODM-based methods performed better for the silicon cells: the monocrystalline and polycrystralline technologies are the ones which most closely conform to the modeling assumptions of the ODM. Hence, it naturally provides an excellent fit to their empirical I-V characteristics. In any case, we must emphasize that the proposed method also yielded good performance for the silicon solar cells, with a current NRMSE not surpassing 2%.

Also compared to the ODM-based methods, it is clear that the proposed method yields much smaller execution times, which has a twofold cause. First, as was established in **Lemma 1**, the optimization variable γ is constrained to the narrow interval $\Gamma \subset [0, 1]$. Hence, it is ensured that a small number of operations will be required for completing the direct search; this is not true for methods [25], [26], [27], since R_s does not have general (i.e, applicable to any solar cell) and well-defined search bounds. Second, during NRMSE evaluation of the ODM-based methods, each $I(V_i)$ in (21) must be obtained by evaluating the Lambert W function to solve the implicit ODM equation [4]. Hence, aside from having a higher operation number (see Section III), the ODM methods have a more time-consuming fundamental operation.

It is interesting to note that $\gamma_{\max}$ bears some influence on execution time of the proposed method. The results clearly show that larger $\gamma_{\max}$ imply greater execution time, which is entirely consistent with the analysis carried out in Section III, where we established a required number of operations equal to $1 + \frac{\gamma_{\max}}{\Delta\gamma}$. The organic cell with titanium oxide layer represents the worst-case scenario of $\gamma_{\max} = 1$ [see Fig. 6(a)], which, as per **Lemma 1**, happens because $V_{mp} < \frac{V_{oc}}{2}$. However, even in this case, the proposed method required 13 ms, which is at least two orders of magnitude below the execution times of the ODM-based methods.

TABLE 3. Performance metrics of each method for the thin-film cell.

Method	Ξ (%)	Z (%)	Ψ (%)	$\lceil T \rceil$ (ms)	MPP fit
Villalva et al. [25]	5.8901	8.0035	6.6581	2140	Inadequate
Vieira and Corrêa [26]	1.9132	3.2788	1.9650	2413	Inadequate
Rhouma et al. [27]	2.2474	3.2488	2.4043	26920	Inadequate
Analytical method [34]	3.1384	5.4482	3.5614	1	Adequate
Proposed method	2.5225	4.9260	2.8139	7	Adequate

TABLE 4. Performance metrics of each method for the organic cell.

Method	Ξ (%)	Z (%)	Ψ (%)	$\lceil T \rceil$ (ms)	MPP fit
Villalva et al. [25]	3.6479	14.5882	5.1198	2542	Inadequate
Vieira and Corrêa [26]	3.5578	19.2682	6.0517	2825	Inadequate
Rhouma et al. [27]	0.0726	0.3390	0.1049	25463	Adequate
Analytical method [34]	1.5329	2.3690	1.5012	1	Adequate
Proposed method	0.3713	1.5679	0.5813	4	Adequate

TABLE 5. Performance metrics of each method for the organic cell with titaninum oxide layer.

Method	Ξ (%)	Z (%)	Ψ (%)	$\lceil T \rceil$ (ms)	MPP fit
Villalva et al. [25]	15.7854	48.4370	45.6812	2874	Inadequate
Vieira and Corrêa [26]	13.5468	48.4555	55.3319	3232	Inadequate
Rhouma et al. [27]	10.5515	38.4997	57.6145	27474	Adequate
Analytical method [34]	1.6057	7.7751	8.5024	1	Adequate
Proposed method	1.4296	7.8788	6.5699	13	Adequate

At last, an important feature of the proposed method is that it avoided the problem of inadequate MPP fit that occurred at least once for each ODM-based method, which is explained as follows. Despite all ODM-based methods using the condition $I(V_{mp}) = I_{mp}$ in their formulations, none of them imposes the condition $\partial_V I(V_{mp}) = -\frac{I_{mp}}{V_{mp}}$, which is responsible for ensuring that $I(V)$ has its maximum exactly at (V_{mp}, I_{mp}). Hence, it is possible for the predicted curve to pass through (V_{mp}, I_{mp}) but not have its maximum at this point. Such considerations are also true for the proposed method, but it compensates for this by fitting (V_{mp}, I_{mp}) *close to the maxima of two orthogonal parabolas* (as seen from Fig. 1), which makes the predicted I-V curve closely approximate the maximum condition $\partial_V I(V_{mp}) = -\frac{I_{mp}}{V_{mp}}$.

All of the foregoing discussion shows that, if ETPQM is used for modeling, it is worthwhile to apply the proposed parameter extraction method if empirical I-V samples are available for NRMSE computations. In fact, it consistently reduces NRMSE with respect to the analytical method [34] and requires negligible processing time. However, if the empirical I-V samples are unavailable, the analytical method remains as a simpler but less accurate alternative.

V. CONCLUSION

A low-complexity search-based parameter extraction method for the ETPQM solar cell I-V characteristic model has been proposed. Its validation was carried out via accuracy and execution time comparisons against the analytical ETPQM parameter extraction and other low-complexity search-based methods from the literature applicable to the ODM. The results proved that the proposed method consistently reduces NRMSE with respect to the analytical method with a very mild execution time trade-off. Furthermore, it is faster than the ODM-based methods and, depending on the considered solar cell, is capable of outperforming them. Hence, it is an effective and easily applicable method for ETPQM parameter extraction and its usage is encouraged if a sampled solar cell I-V curve is available for carrying out NRMSE optimization.

REFERENCES

[1] H. Tian, F. Mancilla-David, K. Ellis, E. Muljadi, and P. Jenkins, "A cell-to-module-to-array detailed model for photovoltaic panels," *Sol. Energy*, vol. 86, no. 9, pp. 2695–2706, Sep. 2012.
[2] W. De Soto, S. A. Klein, and W. A. Beckman, "Improvement and validation of a model for photovoltaic array performance," *Sol. Energy*, vol. 80, no. 1, pp. 78–88, 2006.
[3] R. Messenger and A. Abtahi, *Photovoltaic Systems Engineering*. Boca Raton, FL, USA: CRC Press, 2017.
[4] S. Pindado, J. Cubas, E. Roibás-Millán, F. Bugallo-Siegel, and F. Sorribes-Palmer, "Assessment of explicit models for different photovoltaic technologies," *Energies*, vol. 11, no. 6, p. 1353, May 2018.
[5] A. M. Humada, S. Y. Darweesh, K. G. Mohammed, M. Kamil, S. F. Mohammed, N. K. Kasim, T. A. Tahseen, O. I. Awad, and S. Mekhilef, "Modeling of PV system and parameter extraction based on experimental data: Review and investigation," *Sol. Energy*, vol. 199, pp. 742–760, Mar. 2020.
[6] R. Franco and F. Vieira, "Analytical method for extraction of the single-diode model parameters for photovoltaic panels from datasheet data," *Electron. Lett.*, vol. 54, no. 8, pp. 519–521, 2018.

[7] S. X. Lun, C. J. Du, G. H. Yang, S. Wang, T. T. Guo, J. S. Sang, and J. P. Li, "An explicit approximate I–V characteristic model of a solar cell based on padé approximants," *Sol. Energy*, vol. 92, pp. 147–159, Jun. 2013.
[8] J. Cubas, S. Pindado, and M. Victoria, "On the analytical approach for modeling photovoltaic systems behavior," *J. Power Sources*, vol. 247, pp. 467–474, Feb. 2014.
[9] S. Hara, "Parameter extraction of single-diode model from module datasheet information using temperature coefficients," *IEEE J. Photovolt.*, vol. 11, no. 1, pp. 213–218, Jan. 2021.
[10] H. Saleem and S. Karmalkar, "An analytical method to extract the physical parameters of a solar cell from four points on the illuminated $J--V$ curve," *IEEE Electron Device Lett.*, vol. 30, no. 4, pp. 349–352, Apr. 2009, doi: 10.1109/LED.2009.2013882.
[11] A. Ortiz-Conde, F. J. García Sánchez, and J. Muci, "New method to extract the model parameters of solar cells from the explicit analytic solutions of their illuminated I–V characteristics," *Sol. Energy Mater. Sol. Cells*, vol. 90, no. 3, pp. 352–361, 2006.
[12] L. Peng, Y. Sun, Z. Meng, Y. Wang, and Y. Xu, "A new method for determining the characteristics of solar cells," *J. Power Sources*, vol. 227, pp. 131–136, Apr. 2013.
[13] M. Abdel-Basset, R. Mohamed, S. Mirjalili, R. K. Chakrabortty, and M. J. Ryan, "Solar photovoltaic parameter estimation using an improved equilibrium optimizer," *Sol. Energy*, vol. 209, pp. 694–708, Oct. 2020.
[14] A. A. Cardenas, M. Carrasco, F. Mancilla-David, A. Street, and R. Cardenas, "Experimental parameter extraction in the single-diode photovoltaic model via a reduced-space search," *IEEE Trans. Ind. Electron.*, vol. 64, no. 2, pp. 1468–1476, Feb. 2017.
[15] S. Gude and K. C. Jana, "Parameter extraction of photovoltaic cell using an improved cuckoo search optimization," *Sol. Energy*, vol. 204, pp. 280–293, Jul. 2020.
[16] I. A. Ibrahim, M. J. Hossain, B. C. Duck, and C. J. Fell, "An adaptive wind-driven optimization algorithm for extracting the parameters of a single-diode PV cell model," *IEEE Trans. Sustain. Energy*, vol. 11, no. 2, pp. 1054–1066, Apr. 2020.
[17] S. Jiao, G. Chong, C. Huang, H. Hu, M. Wang, A. A. Heidari, H. Chen, and X. Zhao, "Orthogonally adapted Harris hawks optimization for parameter estimation of photovoltaic models," *Energy*, vol. 203, Jul. 2020, Art. no. 117804.
[18] C. Kumar, T. D. Raj, M. Premkumar, and T. D. Raj, "A new stochastic slime mould optimization algorithm for the estimation of solar photovoltaic cell parameters," *Optik*, vol. 223, Dec. 2020, Art. no. 165277.
[19] R. B. Messaoud, "Extraction of uncertain parameters of single and double diode model of a photovoltaic panel using salp swarm algorithm," *Measurement*, vol. 154, Mar. 2020, Art. no. 107446.
[20] M. Premkumar, T. S. Babu, S. Umashankar, and R. Sowmya, "A new metaphor-less algorithms for the photovoltaic cell parameter estimation," *Optik*, vol. 208, Apr. 2020, Art. no. 164559.
[21] J. P. Ram, T. S. Babu, T. Dragicevic, and N. Rajasekar, "A new hybrid bee pollinator flower pollination algorithm for solar PV parameter estimation," *Energy Convers. Manage.*, vol. 135, pp. 463–476, Mar. 2017.
[22] B. Subudhi and R. Pradhan, "Bacterial foraging optimization approach to parameter extraction of a photovoltaic module," *IEEE Trans. Sustain. Energy*, vol. 9, no. 1, pp. 381–389, Aug. 2017.
[23] Y. Tao, J. Bai, R. K. Pachauri, and A. Sharma, "Parameter extraction of photovoltaic modules using a heuristic iterative algorithm," *Energy Convers. Manage.*, vol. 224, Nov. 2020, Art. no. 113386.
[24] R. Venkateswari and N. Rajasekar, "Review on parameter estimation techniques of solar photovoltaic systems," *Int. Trans. Electr. Energy Syst.*, vol. 31, no. 11, Nov. 2021, Art. no. e13113.
[25] M. G. Villalva, J. R. Gazoli, and E. R. Filho, "Comprehensive approach to modeling and simulation of photovoltaic arrays," *IEEE Trans. Power Electron.*, vol. 24, no. 5, pp. 1198–1208, May 2009.
[26] F. H. T. Vieira and H. P. Correa, "Methods for estimating one-diode model parameters of photovoltaic panels and adjusting to non-nominal conditions," *Adv. Electr. Comput. Eng.*, vol. 19, no. 1, pp. 27–34, 2019.
[27] M. B. H. Rhouma, A. Gastli, L. Ben Brahim, F. Touati, and M. Benammar, "A simple method for extracting the parameters of the PV cell single-diode model," *Renew. Energy*, vol. 113, pp. 885–894, Dec. 2017.
[28] A. K. Das, "An explicit $J--V$ model of a solar cell using equivalent rational function form for simple estimation of maximum power point voltage," *Sol. Energy*, vol. 98, pp. 400–403, Dec. 2013.
[29] A. K. Das, "An explicit $J--V$ model of a solar cell for simple fill factor calculation," *Sol. Energy*, vol. 85, no. 9, pp. 1906–1909, 2011.
[30] T. O. Saetre, O.-M. Midtgård, and G. H. Yordanov, "A new analytical solar cell I–V curve model," *Renew. Energy*, vol. 36, no. 8, pp. 2171–2176, 2011.
[31] M. Akbaba and M. A. Alattawi, "A new model for I–V characteristic of solar cell generators and its applications," *Sol. Energy Mater. Sol. Cells*, vol. 37, no. 2, pp. 123–132, 1995.
[32] S. Pindado and J. Cubas, "Simple mathematical approach to solar cell/panel behavior based on datasheet information," *Renew. Energy*, vol. 103, pp. 729–738, Apr. 2017.
[33] S. Karmalkar and S. Haneefa, "A physically based explicit $J--V$ model of a solar cell for simple design calculations," *IEEE Electron Device Lett.*, vol. 29, no. 5, pp. 449–451, May 2008.
[34] H. P. Corrêa and F. H. T. Vieira, "Explicit two-piece quadratic current–voltage characteristic model for solar cells," *IEEE Trans. Electron Devices*, vol. 68, no. 12, pp. 6273–6278, Dec. 2021.
[35] T. G. Kolda, R. M. Lewis, and V. Torczon, "Optimization by direct search: New perspectives on some classical and modern methods," *SIAM Rev.*, vol. 45, no. 3, pp. 385–482, 2003.
[36] *Full-Square Monocrystalline Solar Cell*, Hanhwa Q Cells, Bitterfeld-Wolfen, Germany, 2013. [Online]. Available: https://www.spectrolab.com/DataSheets/TNJCell/tnj.pdf
[37] T. Easwarakhanthan, J. Bottin, I. Bouhouch, and C. Boutrit, "Nonlinear minimization algorithm for determining the solar cell parameters with microcomputers," *Int. J. Solar Energy*, vol. 4, no. 1, pp. 1–12, 1986.
[38] *26.8% Improved Triple Junction (ITJ) Solar Cells*, Spectrolab Photovoltaic Products, Sylmar, CA, USA, 2008. [Online]. Available: https://www.spectrolab.com/DataSheets/TNJCell/tnj.pdf
[39] T. Jeranko, H. Tributsch, N. S. Sariciftci, and J. C. Hummelen, "Patterns of efficiency and degradation of composite polymer solar cells," *Sol. Energy Mater. Sol. Cells*, vol. 83, nos. 2–3, pp. 247–262, Jun. 2004.
[40] B. Ecker, H.-J. Egelhaaf, R. Steim, J. Parisi, and E. von Hauff, "Understanding S-shaped current–voltage characteristics in organic solar cells containing a TiO_x interlayer with impedance spectroscopy and equivalent circuit analysis," *J. Phys. Chem. C*, vol. 116, no. 31, pp. 16333–16337, 2012.
[41] R. Saive, "S-shaped current–voltage characteristics in solar cells: A review," *IEEE J. Photovolt.*, vol. 9, no. 6, pp. 1477–1484, Nov. 2019.
[42] B. Romero, G. del Pozo, B. Arredondo, D. Martín-Martín, M. P. R. Gordoa, A. Pickering, A. Pérez-Rodríguez, E. Barrena, and F. J. García-Sánchez, "S-shaped $I--V$ characteristics of organic solar cells: Solving Mazhari's lumped-parameter equivalent circuit model," *IEEE Trans. Electron Devices*, vol. 64, no. 11, pp. 4622–4627, Nov. 2017.

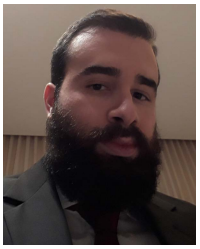

HENRIQUE P. CORRÊA received the bachelor's degree in electrical engineering and the master's degree in electrical and computer engineering from the Federal University of Goiás (UFG), Brazil, in 2017 and 2019, respectively, where he is currently pursuing the Ph.D. degree in electrical and computer engineering. He is also a Federal Employee with the School of Electrical, Mechanical and Computer Engineering, UFG. His main research interests include power distribution networks, photovoltaic systems, and power system optimization.

FIÁVIO H. T. VIEIRA received the bachelor's degree in electrical engineering and the master's degree in electrical and computer engineering from the Federal University of Goiás (UFG), Brazil, in 2000 and 2002, respectively, and the Ph.D. degree in electrical engineering from the State University of Campinas (UNICAMP), in 2006. He is currently an Associate Professor at the School of Electrical, Mechanical and Computer Engineering (EMC), UFG. His main research interests include modeling and control of network traffic, communication networks, computational intelligence, and optimization applied to communication and power systems.